JOURNAL OF MECHANICS OF CONTINUA AND MATHEMATICAL SCIENCES
www.journalimcms.org

ISSN (Online) : 2454 -7190 Vol.-15, No.-11, November (2020) pp 23-35 ISSN (Print) 0973-8975

AN EXTENDED AND UNSCENTED KALMAN FILTERS SIMULATION AND DESIGN FOR A MOBILE ROBOT

Rashid Ali[1], Muhammad Arshad[2]

[1] Lecturer, Dept. of Computer Science University of Turbat, Turbat, Pakistan

[2]MS Scholar, GSESIT, FEST, HUCC, Hamdard University Karachi, Pakistan
[1] rashidcs@uot.edu.pk, [2]arrshadd@gmail.com

Corresponding Author: **Rashid Ali**

https://doi.org/10.26782/jmcms.2020.11.00003

(Received: September 12, 2020; Accepted: October 27, 2020)

Abstract

This research analyzes the design and simulation of a mobile robot using an Extended Kalman Filter (EKF) and an Unscented Kalman filter (UKF). The mobile platform has a differential configuration, where each track of a wheel is associated with an encoder. The EKF and UKF methods are used to integrate the measurements of a novel odometric system based on the optical mice and the measurements of a localization system based on a map of geometric beacons. Two different types of simulations have been performed for validating the results, either using the mouse-based odometric system or using the conventional wheel encoder-based odometric system, to compare and evaluate the errors made by each system.

Keywords: Extended Kalman Filter, Unscented Kalman Filter, localization, odometry, encoder, optical mouse sensor.

I. Introduction

To understand the issue of sensor fusion information for the navigation and localization of the differential-drive mobile robots, it is important to know the navigation and localization of the mobile robots together with the Extended and Unscented Kalman Filters [XVIII]. Mobile robots are designed and simulated with various applications, performing one or several tasks simultaneously. In general, robots navigate in the environment, exploring or following a path with the help of programming. They must avoid possible obstacles until they reach their destination point and communicate with neighboring robots to coordinate their movements or maintain the desired formation [VI]. All these tasks must be carried out autonomously in most cases, for which a control system is implemented at different levels to establish the speeds of the robot wheels necessary to follow the planned trajectory and to reach the destination point.

The estimation of an autonomous mobile robot its localization, position and orientation at every moment constitutes an essential condition for its navigation. Traditionally, differential drive robots are located using incremental methods, such as

odometry. Its main drawback lies in the accumulation of errors along the path, being necessary to develop systems correction, which acts periodically at certain points of an environment [XVIII]. Such correction methods may consist of the use of localization systems that are integrated with incremental odometry.

The process of localizing a mobile robot through a beacon system requires prior knowledge of the positions in which the emitters are located within the map. The integration of the localization system and the odometry system has been carried out through the extended and unscented Kalman filters [III] [XXII] [VII] in the present work. A recursive method which allows us to obtain an estimated value for the minimum variance of the state based on inaccurate observations.

The following describes the test platform on which the filters are intended to be implanted, as well as the odometry and localization systems used in the simulation. In general, the EKF and UKF are presented in equations for the characteristics of the mobile platform to the odometry and the localization data provided by the corresponding systems.

II. Description of the Platform Test

The platform on which the simulation tests have been performed to present the differential-drive mobile robot position and direction. Its locomotion system is formed by diametrically opposite wheels located on an axis perpendicular to the robot [XXIII]. Each of the rear wheels has a motor equipped so that the turns are made by giving different speeds to each of the wheels. To keep the system in its direction, the wheels, with the help of optical mice and encoders, are used anonymously [VIII]. The structure of the locomotion system is shown in Figure 1. Two 12 voltage batteries power the motor, and the two encoders are attached to the wheel motors, which could be used to implement the odometric system. However, the odometric information is provided by another less conventional system that uses two optical mice that measure the increases in displacements that the robot experiences. The localization of the differential drive mobile robot is done through a set of beacons located along with the environment of the robot, and a beacon decoding system is also equipped with the same platform [XX].

In the following sections, each of the systems is described in detail.

Odometric System

An optical mouse sensor allows us to know its position and movement direction relative to some axes associated with the mouse and coincide with its longitudinal and transverse axis, i.e. q and r as given in Figure 2. The odometer system is made up of two optical mice that will calculate the increases in the position of the platform, referred to as a fixed reference system, i.e. x and y axes. But being an incremental system, the accumulation of errors throughout the movement can produce a considerable error when estimating the global position of the platform [XIV]. In Figure 2, you can see a scheme in which the increments measured by each mouse are represented in case of changing position and its direction.

On the platform, the position of the mouse 1 coincides with the position of the location system. Therefore, we are interested in knowing the position of point 1 in the global reference system given by the odometry system. This position is calculated by integrating the different measures that the mouse placed at that point, which performs. Thus the position is calculated with Eq. (1), (2) and (3) with the help of a global reference system.

$$x_1^{'} = x_1 + (\sqrt{\Delta r_1^2 + \Delta q_1^2})\, cos(\emptyset_k + arctan(\tfrac{\Delta r_1}{\Delta q_1})) \tag{1}$$

$$y_1^{'} = y_1 + \left(\sqrt{\Delta r_1^2 + \Delta q_1^2}\right) sin\left(\emptyset_k + arctan\left(\frac{\Delta r_1}{\Delta q_1}\right)\right) \tag{2}$$

The orientation of the robot will be:

$$\Delta\emptyset = arcsin\left(\frac{\Delta r_1 - \Delta r_2}{L}\right) \tag{3}$$

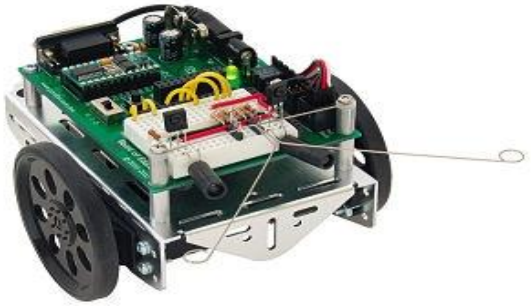

Fig 1. Real system differential structure of a mobile robot.

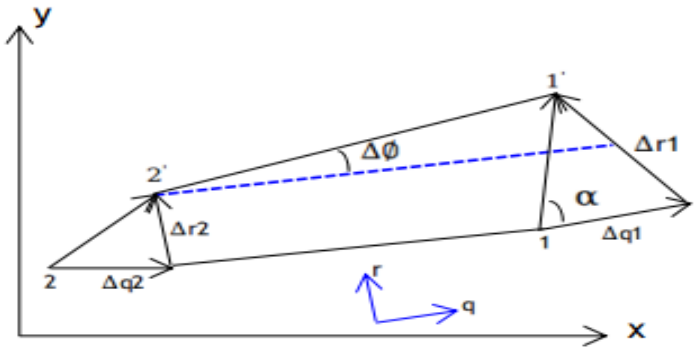

Fig 2. Measurement of Odemetry system

Localization System

The localization system consists of a series of beacons that are distributed throughout the environment in which the robot moves; the position of each of them is being known. The beacons, when excited by a rotating laser located in the robot, emit a code that is known by the decoder [IX]. Upon receiving the code of the beacon, the decoder calculates the angle with which said beacon is seen and sends all this information by the serial port to the PC along with the instant at which the measurement was made. Accelerations are measured using two encoders placed on each robot wheel, as in the previous case.

Upon receiving this information, the PC searches the history of received beacons for the two closest beacons at least 90 degrees from the angle of the received beacons, in figure 3 beacons 2 and 3 are used to triangulate so that the position of the platform with reference to the global system is obtained. A scheme that summarizes the triangulation process appears in Figure 3. The way to obtain the position of the robot through triangulation, when a beacon is received, In Figure 3(a) the angle at which the beacon is seen from the robot, and the history of received beacons is used to find the beacon closest to one of the orthogonal angles to the received one [V], [XV]. The angular difference in figure 3(b) with which both beacons are seen defines a capable arc on which the actual position of the robot is known. Repeating the same process with the other orthogonal angle is another capable arc which is shown in figure 3(c). The intersection of both defined two points, one of which is the mobile robot position and the other is the new received beacon position where shown in figure 3(d).

Once the measurements of the localization system and the odometry system have been obtained, they must be integrated through the extended and unscented Kalman filters, whose formulation is described in the following section.

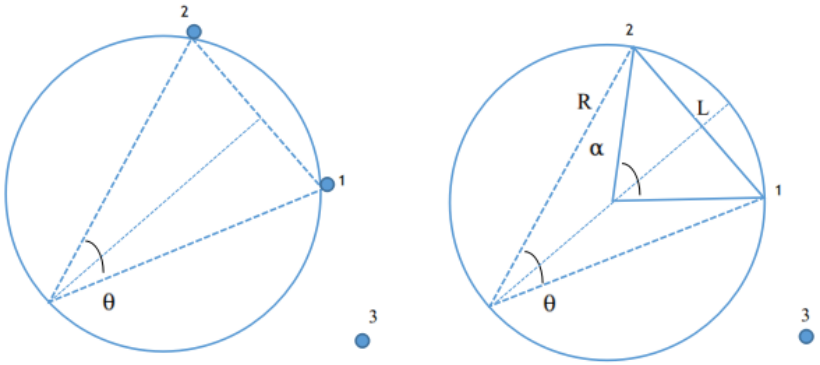

(a) (b)

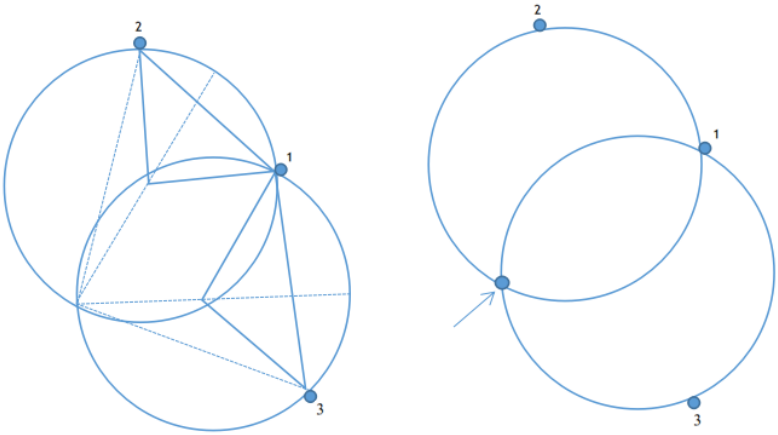

(c) (d)

Fig 3. Localization system estimations (a) the beacon angle and the robot (b) the angular difference of both beacons and the actual position of the robot (c) orthogonal angle process (d) mobile robot and the new beacon position

III. Extended and Unscented Kalman Filters

The discrete EKF [IV] is used to link the position measurements of the ode-metric and localization system. The general equations of the EKF are particularized to the mobile platform that has been described below.

In general, it is based on a non-linear system that responds to equation (4) and a measurement system. According to equation (5), where x_k and z_k represent in the state vector and the measurement of that vector at the moment k,$f(.)$ and $h(.)$ are non-linear functions; that model the operation of the real system and the measurement system, u_k is the input of the system, w_{k-1}represents the system error, and y_{k-1} the input disturbance and v_{k-1} the measurement noise:

$$x_k = f(x_{k-1}, u_k, w_{k-1}, \gamma_{k-1}) \quad (4)$$

$$z_k = h(x_k, v_{k-1}) \quad (5)$$

By eliminating the noise from the previous equations and representing them in terms of their probability, the estimated state and localization system measurement equations (6) and (7) are obtained as:

$$\hat{x}_k = f(x_{k-1}, u_k, 0, 0) \quad (6)$$

$$\hat{z}_k = h(x_k, 0) \quad (7)$$

The system error, the input disturbance and the noise measurement are supposed to have zero mean and covariance matrix Gaussian distribution Q, Γ and Respectively, therefore its probability distribution will be given by the normal distribution [II].

$$p(w) = N(0, Q) \tag{8}$$

$$p(\gamma) = N(0, \Gamma) \tag{9}$$

$$p(v) = N(0, R) \tag{10}$$

The extended Kalman filter predicts the following system status $\hat{x}_k^-$ based on the available information of the $f(.)$Model and the expected covariance matrix P_k^-. To make this estimate, the propagation equations (11) and (12) are used.

$$\hat{x}_k = f\left(x_{k-1,} u_{k,} 0, 0 \right) \tag{11}$$

$$P_k^- = A_{k,} P_{k-1,} A_k^T + B_k \Gamma_{k-1} B_k^T + Q_{k-1} \tag{12}$$

Once the z_k measures are available, you can proceed to the update stage and calculate the earnings matrix of the Kalman $k_{k,}$filter (13).

The measure can be incorporated into the estimated state $\hat{x}_k$, besides the value of the covariance matrix (15) is updated according to the following equations:

$$K_k = P_k^- H_k^T (H P_k^- H_k^T + R_{k-1})^{-1} \tag{13}$$

$$\hat{x}_k = \hat{x}_k^- + K_k (z_k - h(\hat{x}_k^-, 0)) \tag{14}$$

$$K_k = (I - K_k H_k) P_k^- \tag{15}$$

On the base of UKF, the Unscented Transformation (UT) is used the mathematical process by calculating the estimation of the mean and covariance of the probability distribution of a random variable to which a non-linear transformation has been applied [IV], [X]. To do this, using (sigma points) a series of samples that are generated by the non-linear function we have used [XIII]. The placement of these sigma points is carried out so that, when transforming them, their mean and covariance are as close as possible to those of the original distribution.

Below we have described the method for calculating the sigma points and some weights that helped us in later weight; the extension of these points contributed to the final result [XVII]. We started by defining the sigma points as,

$$x_{k-1|k-1}^0 = X_{k-1|k-1} \tag{16}$$

$$x_{k-1|k-1}^i = X_{k-1|k-1} + (\sqrt{(L + \lambda) P_{k-1|k-1}})_i, \quad i = 1, \ldots, L \tag{17}$$

$$x^i_{k-1|k-1} = X_{k-1|k-1} + (\sqrt{(L+\lambda)P_{k-1|k-1}})_{i-L},$$

i.e. $i = L+1,\ldots,2L$ (18)

Where L is the number of variables that are defined the state of our system, or in other words, the length of vector X, and λ is known as a scale factor and is defined as:

$$\lambda = \alpha^2(L+k) - L \quad (19)$$

α determines the dispersion of the sigma points and usually takes a small value, in our case $\alpha = 10^{-3}$, and k is a second scale parameter that usually takes the value 0. the formula $(\sqrt{(L+\lambda)P_{k-1|k-1}})_i$ represents the column i of the square root matrix of $(L+\lambda)P_{k-1|k-1}$. This matrix is commonly calculated using the so-called Cholesky factorization that allows us to obtain a matrix L from a matrix A so that $A = LL^T$. This is possible to the fact that P is defined as positive and hermetic in case of real and symmetric. In C++, we carried out this decomposition as $L = chol(A)$. It is important to transpose because the program returns L^T. To calculate the weights mentioned above we used the following formulas:

$$W_s^0 = \frac{\lambda}{L+\lambda} \quad (20)$$

$$W_c^0 = \frac{\lambda}{L+\lambda} + (1-\alpha^2-\beta) \quad (21)$$

$$W_s^i = W_c^i = \frac{\lambda}{2(L+\lambda)}, \quad i = 1,\ldots..,2L \quad (22)$$

Where the W_s^i are the weights for the calculation of the state estimate and the measure, W_c^i are the weights for calculating the covariance matrices. Additionally, β is a parameter for integrating prior knowledge of X's distribution. In the case of Gaussian distribution, $\beta = 2$ is the optimum [XI].

IV. Simulations and Results

After obtaining the mathematical expressions of all the equations involved in the filters, we proceed to the next stage in the design of the EKF and UKF. This new stage consists of simulating the filters according to similar operating conditions to those found in the real system [XXI]. The simulation stage must be before the implementation in the real system to debug and adjust the possible problems that the filter presents. [XXIII] To simulate the mobile, it is necessary to define a series of characteristics, such as: 1) An error in the localization system in a maximum position of 4.5 cm is assumed. 2) The maximum error of the orientation localization system is approximately 1.6°. The maximum error of the odometric system is 3 mm. It is assumed that 5 measurements of the odometric system are taken before having a measurement of the localization system. From these assumptions, the simulation is

performed. The results show that the filters are capable of adjusting the position of the robot as shown in Figure 4, making a small error from the odometry and localization data.

The figures showed how the position of the robot calculated through the EKF and UKF practically coincides with the robot's real position accordingly. In Figure 5, the estimated error better over performed and made by the filters, where it can be seen that the maximum error made in position measurement is about 15 cm., And as an average, the error in absolute value is about 3.64 cm in x and 4.26 cm in y respectively. The position error is around 0.50°, and the absolute value for the average error is about 0.127°.

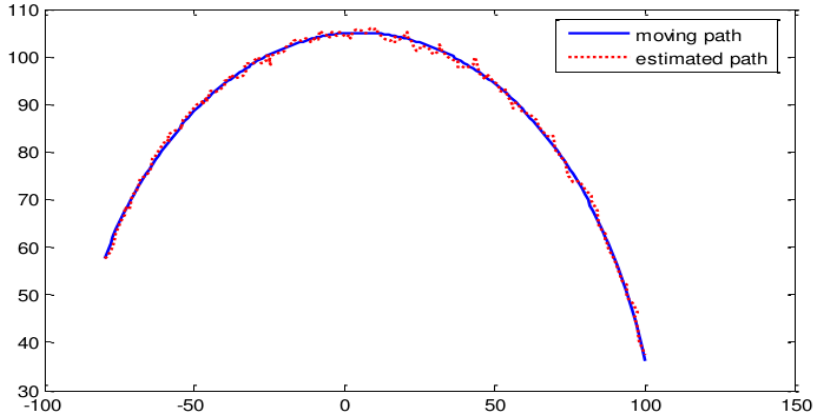

X-location

Fig 4. The orientation and real position (blue) moving path versus position and orientation (red) of the estimated path.

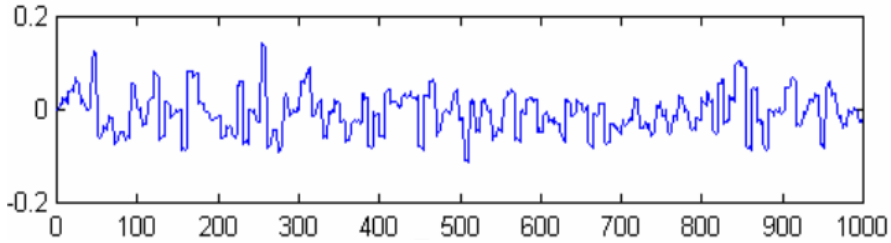

Error in X

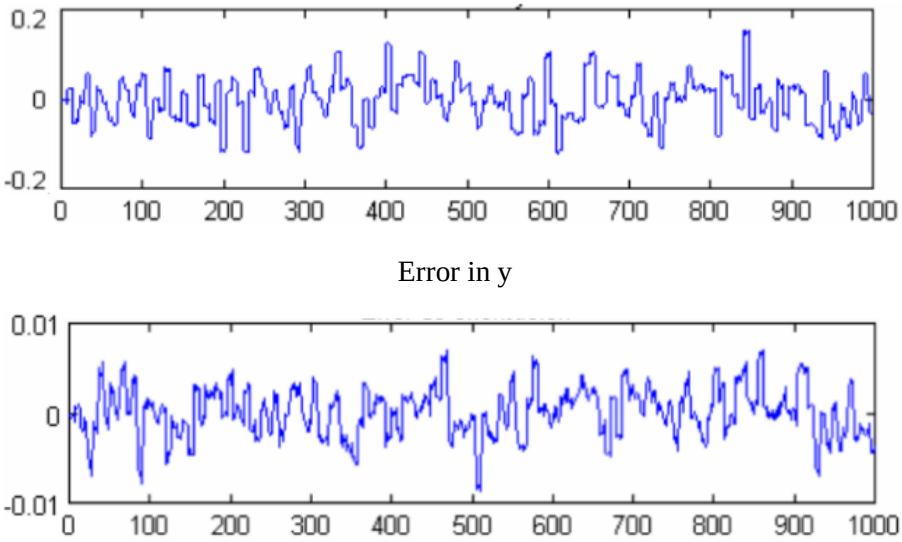

Fig 5. Errors made by the EKF and UKF

These errors are being seen from the localization system, which shows in figure 5 is around 20 cm, and the mean of its absolute value is 8.22 cm in x, 13.2 cm in y and the orientation is about 0.376° accordingly. Comparing these data with the errors made by the filters, it can be seen how the errors decrease the localization system when integrating its measurements with those of the odometric system. Odometry data is used to calculate the position at those times when the beacon system does not provide the measurement. Once a location measurement is obtained, and the odometric position is corrected, thus eliminating the accumulation of error inherent to the integration of its displacements.

To analyze the positioning system as a whole, the filters will be compared with another localization system that uses traditional odometry, that is, based on encoders placed on the wheels. In this case, the equations of motion of the system change slightly [XVI], [XIX] concerning equations (19), (20) and (21).

$$x_{k+1}^{'} = x_k + (\Delta D)cos(\emptyset_k + \Delta\emptyset) \quad (23)$$

$$y_{k+1}^{'} = y_k + (\Delta D)sin(\emptyset_k + \Delta\emptyset) \quad (24)$$

$$\Delta\emptyset_{k+1} = \emptyset_k + \Delta\emptyset \quad (25)$$

With,

$$\Delta D = \frac{\Delta wr + \Delta wl}{2} \text{ and } \Delta\emptyset = \frac{\Delta wr - \Delta wl}{l}$$

Where Δwr and Δwl is the displacement of the right wheel and the left wheel, respectively, and l is the separation between the driving wheels. To compare

these results, the errors made with both odometric methods are compared in Figure 6. The mean error in x,y is 19.15 cm, 15.36 cm, respectively, and the orientation is 1°. In this case, the EKF and UKF in Figure 6 are used together with the non-linear transformation to estimate the robot position, i.e. x, y, θ. This scheme merges the optical mice and encoders by using a complex model that requires a large matrix inversion to calculate the filters gain and the state estimation. Also, it has the advantage that it directly propagates the uncertainty to the position.

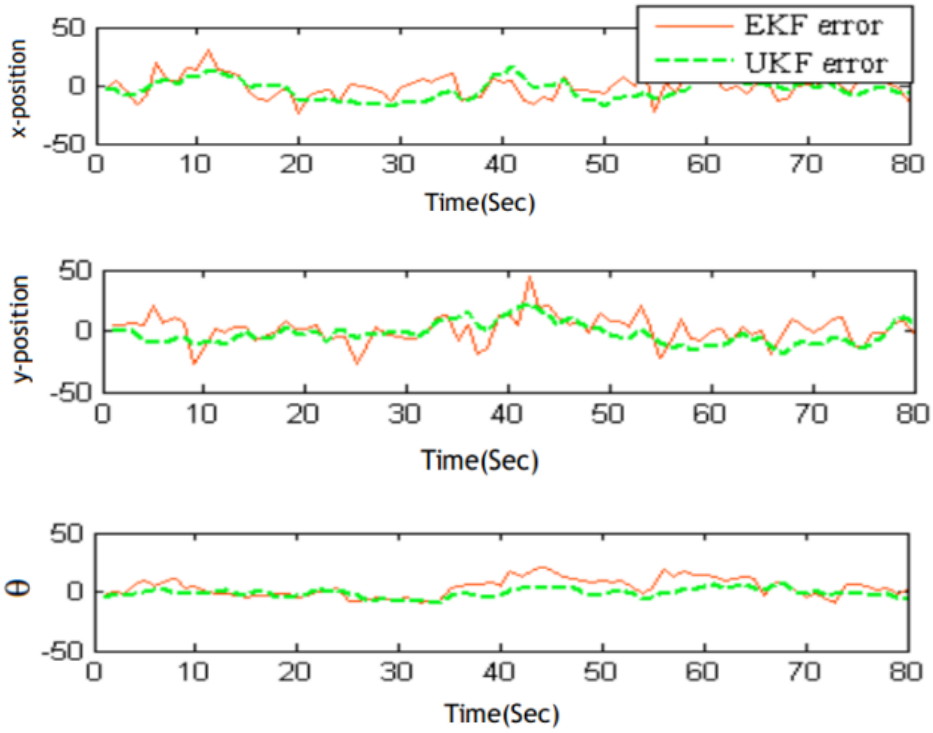

Fig 6. Errors of the system with traditional odometry (green) versus the errors made by the system with odometry implemented through optical mice(red).

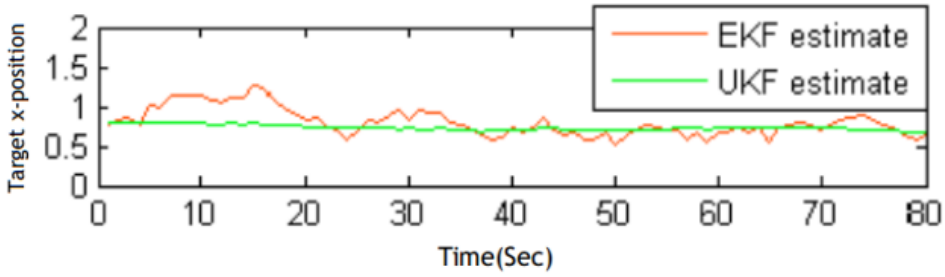

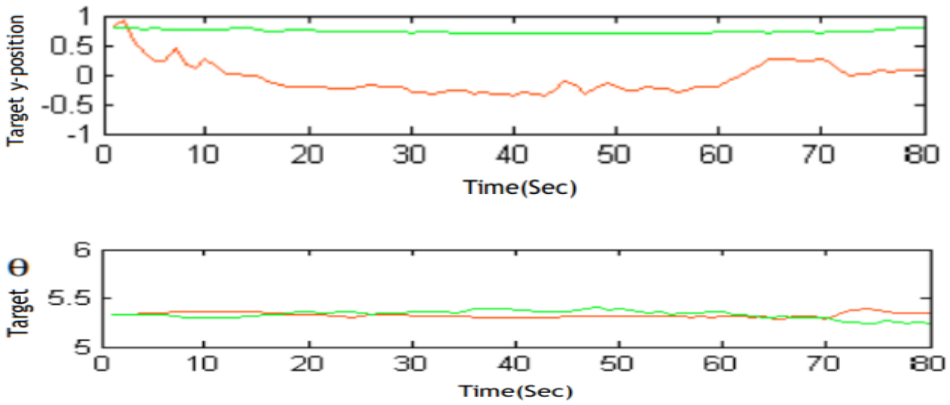

Fig 7. Trajectory system estimations of EKF and UKF

As a result of this comparison, it is concluded that the odometric system is implemented with two optical mice leads to smaller position errors than that used by traditional encoder-based odometry. The trajectory estimations of extended and Unscented Kalman filters show the two wheels' mobile robot [II]. We illustrated the approximated and targeted position for the available measurements of the evaluated performance of EKF and UKF in Figure 7. Furthermore, it outperforms EKF and reveals based on UKF. Therefore, it is justified in that figures that UKF is better than the EKF, the filters show in figure 6 identifies the error comparison. EKF estimated parameters show the values in figure 7. it can be achieved that the UKF is more trusted with the better result in case of nominal values than the EKF.

V. Conclusion

In this article, the results of the simulations carried out on the movement of a real platform that integrates an odometric system based on the use of optical mice have been presented. Localization of the system is performed through integration with the EKF and UKF of localization and odometry measurements. Simulating the system gives results that reflect the errors made by the localization system are within the admissible margins. The mean of the absolute value of the error is 8.22 cm in x, 13.2 cm in y and 0.376° in orientation. These errors, within the admissible margins, are smaller than those made by the odometry or localization system separately. To validate these results, they are compared with the results obtained with those of another identical system that works in parallel, but which integrates a traditional odometry system formed by encoders associated with the wheels. In this case, the mean error in x is 19.15 cm, in y is 15.36 cm and 1° in orientation. These errors are greater than those that occurred with the new odometric system, so it seems logical to think that the design and implementation of the filters in the real system produces better results than the simple use of odometry or localization separately. On the other hand, the new odometric system based on the use of optical mouse sensors presents fewer errors than the traditional encoder-based odometry system.

Conflict of Interest:

Authors declared : No conflict of interest regarding this article

References

I. Antonelli,G. and S.Chiaverini,. Linear estimation of the physical odometric parametric parameters for differential-drive mobile robots. Springer Netherlands, Auton Robots, 23:59-68. 2007.

II. B. Subhojyoti, K. Amit, and P. Gupta, "On the noise and power performance of a shoe-mounted multi-IMU inertial positioning system," in Proceedings of the International Conference on Indoor Positioning and Indoor Navigation (IPIN 2017), Sapporo, Japan, September 2017.

III. Cui, M., Liu, W., Liu, H., et al.: Extended state observer-based adaptive sliding mode control of differential-driving mobile robot with uncertainties. Nonlinear Dyn. 83(1–2), 667–683 (2016)

IV. Chen, X. et al. A novel UKF based scheme for GPS signal tracking in high dynamic environment. Proc. of 3rd International Symposium on Systems and Control in Aeronautics and Astronautics (ISSCAA), Harbin, 2010, pp. 202-206.

V. Cimino, Mauro, and Prabhakar R. Pagilla. "Location of optical mouse sensors on mobile robots for odometry." 2010 IEEE International Conference on Robotics and Automation. IEEE, 2010.

VI. Denis F. Wolf, Gaurav S. Sukhatme, "Mobile robot simultaneous localization and mapping in dynamic environments," Autonomous Robots, vol. 19, no. 1, pp. 53-65, July 2005.

VII. Dahmen, H.; Mallot, H.A. Odometry for ground moving agents by optic flow recorded with optical mouse chips. Sensors 2014, 14, 21045–21064.

VIII. Dong, W.: Tracking control of multiple-wheeled mobile robots with limited information of a desired trajectory. IEEE Trans Robot. 28(1), 262–268 (2012)

IX. Doh NL, Choset H and Chung WK . "Relative localization using path odometry information", Autonomous Robots. 21: 143-154.(2006)

X. F. Wang, Y. Lin, T. Zhang, and J. Liu, "Particle filter with hybrid proposal distribution for nonlinear state estimation," Journal of Computers, vol. 6, no. 11, pp. 2491–2501, 2011.

XI. Houshangi, Nasser, and Farouk Azizi. "Mobile Robot Position Determination Using Data Integration of Odometry and Gyroscope." 2006 World Automation Congress.

XII. Iman Abdalkarim Hasan, Nabil Hassan Hadi, : ADAPTIVE PI-SLIDING MODE CONTROL OF NON-HOLOMONIC WHEELED MOBILE ROBOT, J. Mech. Cont.& Math. Sci., Vol.-15, No.-2, February (2020) pp 236-25.

XIII. Kim, S.; Lee, S. Robust velocity estimation of an omnidirectional mobile robot using a polygonal array of optical mice. In Proceedings of the IEEE International Conference on Information and Automation, Changsha, China, 20–23 June 2008; pp. 713–721.

XIV. Lee D and Chung W (2006) Discrete-Status-Based Localization for Indoor Service Robots, IEEE Transactions on Industrial Electronics. 53: 1737-1746.

XV. Lee, Wei-chen, and Cong-wei Cai. "An orientation sensor for mobile robots using differentials." International Journal of Advanced Robotic Systems 10.2 (2013): 134.

XVI. Pozna, C., Troester, F., Precup, R.-E., Tar, J.K., Preitl, S.: On the design of an obstacle avoiding trajectory: method and simulation. Math. Comput. Simul. 79(7), 2211–2226 (2009).

XVII. Rao S K, Kumar D V A N R and Raju K P 2013 Combination of pseudo-linear estimator and modified gain bearings-only extended Kalman filter for passive target tracking in abnormal conditions. Ocean Electron. (SYMPOL) p 3–8.

XVIII. Sousa, A.j., P.j. Costa, A.p. Moreira, and A.s. Carvalho. "Self Localization of an Autonomous Robot: Using an EKF to Merge Odometry and Vision Based Landmarks." 2005 IEEE Conference on Emerging Technologies and Factory Automation.

XIX. S. Kosanam and D. Simon, "Kalman filtering with uncertain noise covariances," in Proceedings of the Intelligent Systems and Control (ISC '04), pp. 375–379, Honolulu, Hawaii, USA, 2004.

XX. Tovar, Benjamin, and Todd Murphey. "Trajectory Tracking among Landmarks and Binary Sensor-beams." 2012 IEEE International Conference on Robotics and Automation (2012)

XXI. TesliÄ , Luka, Igor Å krjanc, and Gregor KlanÄ ar. "EKF-Based Localization of a Wheeled Mobile Robot in Structured Environments." Journal of Intelligent & Robotic Systems 62.2 (2010):187-203.

XXII. Ullah, I., Ullah, F., Ullah, Q., Shin, S.: Integrated tracking and accident avoidance system for mobile robots. Int. J Integrated Control Autom. Syst. 11(6), 1253–1265 (2013)

XXIII. Uyulan, C., Erguzel, T. and Arslan, E., 2017, September. Mobile robot localization via sensor fusion algorithms. In 2017 Intelligent Systems Conference (IntelliSys) (pp. 955-960). IEEE.

XXIV. Wang, Z.P., Ge, S.S., Lee, T.H.: Adaptive neural network control of a wheeled mobile robot violating the pure nonholonomic constraint. In: Proceeding of the IEEE International Conference on Decision and Control, p. 51985203 (2004).

XXV. Younus Kawther K, Nabil H Hadi, : OPTIMUM PAATH TRACKING AND CONTROL FOR A WHEELED MOBILE ROBOT (WMR), J. Mech. Cont.& Math. Sci., Vol.-15, No.-1, January (2020) pp 73-95.